

Modeling of Wear in a Solid-Lubricated Ball Bearing[©]

PRADEEP K. GUPTA (Member, ASLE)

PKG Incorporated

Clifton Park, New York 12065

and NELSON H. FORSTER

Air Force Wright Aeronautical Laboratories

Wright-Patterson Air Force Base, Ohio 45433

Computer modeling of wear in a solid-lubricated ball bearing for high-speed turbine applications is considered in terms of local interactions and the overall dynamics of the bearing elements. With prescribed coefficients of wear at the various interfaces between the interacting bearing elements, the computer model ADORE is used to obtain the time-averaged wear rates for the balls, races, and the cage as a function of the operating conditions typical of a gas turbine application. The model presents analytical estimates of wear in the ball pockets and at the guide lands of the cage, and it provides some guidance for optimizing cage design in solid-lubricated ball bearings.

INTRODUCTION

The increasing demand for high-operating temperatures of advanced gas turbines has generated a significant interest in the development of solid-lubricated rolling bearings for the main shaft support. At the anticipated temperature levels, in the neighborhood of 700°C, the problems associated with both the materials development and bearing design are significant. Effective bearing performance modeling techniques are required to design the bearing for prescribed materials behavior and provide guidance for the development of the future bearing materials and solid lubricants. In fact, a very close coupling between bearing performance modeling and the materials development is essential for the development of the required bearing technology.

Solid lubricants in rolling bearings can be applied in several forms; low friction coatings on the bearing surfaces, a sacrificial cage which supplies the solid lubricant in the form of a transfer film as the balls collide back and forth in the cage pocket, and a controlled spray of solid lubricant in a powder form are some of the techniques being considered. In all cases, a realistic modeling of wear of bearing elements is necessary in order to accomplish the required material

transfer and the specified bearing life. Aside from the adverse operating conditions, the interaction between bearing elements is greatly complicated by the intricate dynamics as a function of the transfer and frictional behavior of the solid lubricant. For example, for a prescribed bearing geometry, the tractive behavior at the ball/race interface determines the ball/cage collision force which, in turn, controls wear in the cage pocket. As the cage pocket wears, the sacrificial cage will release the solid lubricant and result in a change in pocket clearance which feeds back into the overall dynamics of the cage. The primary objective of the present investigation is, therefore, to present a modeling technique which provides the necessary coupling between the complex dynamics of the bearing elements and the constitutive behavior of the materials determined by conventional friction and wear tests.

Over the past two decades, the modeling techniques for the performance of rolling bearings has been significantly advanced. The conventional quasistatic equilibrium models have been replaced by truly dynamic models which provide a real-time simulation of ball bearing performance by integrating the classical differential equations of motion of the various bearing elements (1)–(5). A recent model, ADORE (5), has been selected as the base model for the present investigation. ADORE models the influence of ball/race traction on the dynamics of the balls and the cage; the tractive forces and expected wear rates at the ball/race interface are determined by greatly refined numerical quadrature; motion of the cage is considered with all six degrees of freedom with discrete models for the interaction at the ball/cage and cage/race interface; and, the integration of the differential equations of motion over extensive time domains is efficiently accomplished by the recently advanced numerical algorithms developed by Fehlberg (5).

Although the feasibility of the dynamic modeling techniques for the performance simulation of ball bearings has been greatly demonstrated (4), (7), (8), the problem of wear prediction still requires significant development. The work presented in this paper provides a first step in terms of coupling the fundamental wear behavior with the overall dynamics of the bearing to arrive at meaningful steady-state

wear rates which can be used for bearing design. The general approach used employs a constitutive wear equation to determine the instantaneous wear rate, at a prescribed time, at any interaction in the bearing, which is defined by the classical equations of motion of the bearing elements; these rates are then time-averaged over the length of simulation. Thus, steady-state rates for the prediction of wear are derived by carrying out a dynamic simulation of the motion of bearing elements over extensive time domains. Since the extent of interaction between bearing elements progressively increases in the event of an instability, such modeling techniques, aside from wear prediction, greatly simplify the process of identification of an instability associated with a particular bearing element. It is, therefore, anticipated that the modeling technique presented herein has a significant design potential.

MODELING APPROACH

The classical wear rate at a concentrated contact is defined by a constitutive wear equation as a function of load, sliding velocity, and properties of the materials in contact. A number of such relationships are available in the literature; with particular emphasis on solid lubricants, the work by Mecklenberg (9) is well noted. Any of these wear relationships may be equally used in the approach presented below; for the purpose of simplicity, however, the validity of the basic approach is demonstrated for the well-known Archard's wear equation:

$$w = K \frac{QV}{H}$$

where w is the instantaneous wear rate, K is the Archard's wear coefficient, H is the hardness of the material, Q and V are, respectively, the instantaneous load and sliding velocity.

The wear coefficient K is determined by conventional wear test, the hardness H is defined for the prescribed materials, the load Q and sliding velocity V are determined at each interaction in the bearing by solving the equations of motion of bearing elements as a function of the operating conditions, bearing geometry, and the traction or frictional behavior at the ball/race, ball/cage, and cage/race contacts. Such solutions for the load and sliding velocities are readily provided by the computer program ADORE (5).

For the ball/race interaction, since the load and sliding velocity greatly vary across the elliptical contact zone, it is necessary to replace the QV term by the integral

$$QV = \iint p v \, dx \, dy$$

where p is the local pressure, v is the local sliding velocity at any point in the contact zone, and the integration is carried out over the contact ellipse.

For a hertzian pressure distribution, the above double integral can be reduced to a numerical quadrature formula based on Chebychev polynomials (5). Also, if the contact ellipse is substantially narrow (the major half-width \gg minor

half-width) the above double integral may be reduced to a single integral with a reasonable approximation; in such a case, Gaussian quadrature may be used to compute the integral, however, significant care in treating the step change in sliding velocity, if any, must be exercised.

For the ball/cage and cage/race interaction, the sliding velocity is normally very large and the size of the contact zone is quite small. It is, therefore, reasonable to consider the interaction as a point contact and use Archard's equation directly to compute the instantaneous wear rate.

Once the wear rate is known at any time, T , during the performance simulation, it is convenient to define a time-averaged wear rate, W , as

$$W(T) = \frac{1}{T} \int_0^T w(t) \, dt$$

Such a time-averaged wear rate will generally stabilize to a steady-state value as the simulation time T increases. For the ball/race contact, if the ball always contacts the races, the wear rate, depending on the applied load, may stabilize rather rapidly. For the ball/cage interaction, however, since the interaction is normally in terms of a collision over a very short time interval, the wear rate will demonstrate a jump at the time of collision and a hyperbolic decay during the time of no contact. As the time of simulation increases and if the motion of the cage is stable, the level of collision forces shall gradually reduce and the time-averaged wear rate shall asymptote to a steady-state value. The behavior at the cage/race interface may be similar if the interaction consists of intermittent contact; in the case of a relatively steady contact, however, the wear rates may stabilize relatively rapidly.

Once the time-averaged wear rates, as defined above, are obtained at each interaction in the bearing, prediction of wear over the prescribed duty cycle of the bearing shall be possible. For the cage, a distribution of wear in each pocket and at the guide lands may be predicted and thus significant guidance to material transfer may be obtained. Such insight shall be significant to the design of solid-lubricated ball bearings.

The primary input to the above formulation is the wear coefficient K , which is normally derived from experimental data. However, since the time-averaged wear rate is directly proportional to the wear coefficient, it is adequate to compute the time-averaged wear rates for any arbitrary wear coefficient and prorate the results for a particular wear coefficient. Such a simplification may not be possible for other more complex wear equations, e.g., Mecklenberg (9), Meeks and Bohner (10), and others, where the wear rate may not vary linearly with the load and sliding velocity.

BEARING GEOMETRY AND OPERATING CONDITIONS

An angular contact ball bearing in the operating environment of high-speed gas turbines is considered. The bearing is assumed to have silicon nitride balls and M50 steel races, while the solid lubricant is supplied by the sacrificial cage which is assumed to be made of a fiber-reinforced composite impregnated with a solid lubricant. Table 1 de-

TABLE 1—BEARING GEOMETRY AND MATERIAL PROPERTIES					
Number of Balls	= 12				
Ball Diameter	= 7.8125 mm				
Pitch Diameter	= 42.8000 mm				
Contact Angle	= 26.50 degrees				
Outer Race Curvature Factor	= 0.5170				
Inner Race Curvature Factor	= 0.5220				
Bearing Bore	= 30 mm				
Bearing Outside Diameter	= 55 mm				
Outer Race Fit	= 0.0025 mm				
Inner Race Fit	= 0.0025 mm				
Cage Outside Diameter	= 46 mm				
Cage Inside Diameter	= 40 mm				
Cage Width	= 12 mm				
Guide Land Clearance (Inner Race)	= 0.250 mm				
Pocket Clearance	= 0.250 mm				
ELEMENT	MATERIAL PROPERTIES				
	DENSITY Kg/M**3	ELASTIC MODULUS N/M**2	POISSON'S RATIO	HARDNESS N/M**3	WEAR COEFF.
Ball	3200	3.10E+11	0.260	1.00E+10	5.00E-06
Races	7750	2.00E+11	0.250	7.84E+09	5.00E-06
Cage	1500	1.73E+09	0.300	1.00E+09	1.00E-05

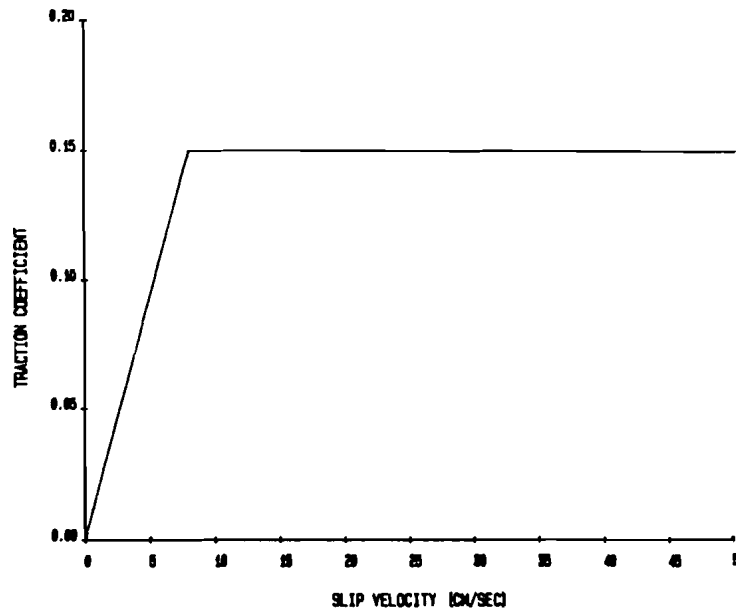


Fig. 1—Model for ball/race traction

describes the geometrical details and properties of the bearing materials. The assumed traction model at the ball/race interface is shown in Fig. 1. The traction coefficient increases linearly with the slip up to a maximum value of 0.15. Such a behavior has been substantiated earlier by Gupta (7) for a typical solid lubricant. In view of the high sliding velocities at the ball/cage and cage/race interfaces, a constant coefficient of friction is assumed to simulate the frictional behavior at these contacts. In order to investigate the effect of pocket and guide land friction on the overall motion of the cage, two values of this friction coefficient, 0.15 and 0.05, are considered.

The bearing is assumed to operate at a shaft speed of

63 500 rpm with an applied thrust load of 1000 N and a synchronous radial load of 500 N.

RESULTS

For the prescribed operating conditions, the dynamic performance of the bearing is simulated over extensive time interval to cover a large number of shaft revolutions and obtain reasonable steady-state solutions. The general load variation at the ball/race contacts, as simulated by ADORE, is shown in Fig. 2*. The sinusoidal variation in contact loads

*All figures are as produced by ADORE. The parameters M and S printed on the right of the figures represent the mean and standard deviation of the plotted solution.

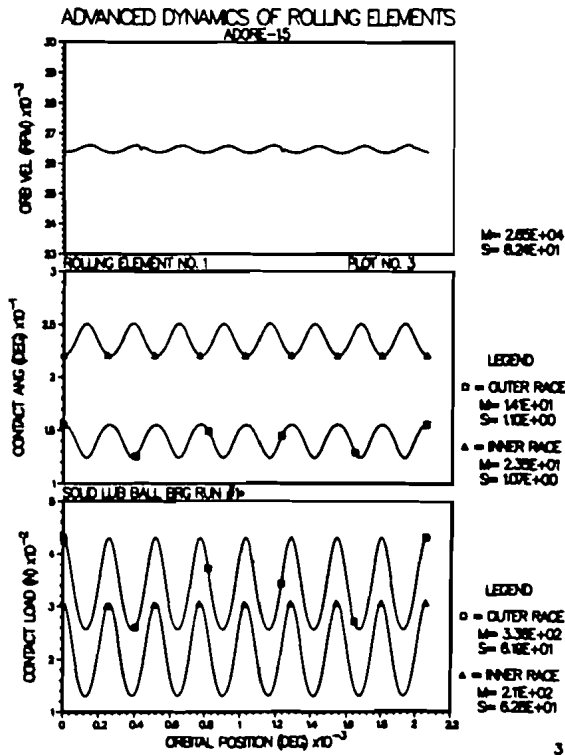


Fig. 2—The variation of ball/race contact loads and angles

and angles result from the combined thrust and radial load. Note that, due to the rotating radial load on the bearing, the frequency of contact load variation is somewhat larger than once per revolution of the ball center along its orbit. Both the angular velocity of the ball and the orbital velocity of its mass center are fairly constant, except for a small sinusoidal variation due to the variable load.

The collision forces in the ball pockets are highly transient; both the magnitude of force and duration of contact are functions of time. Figure 3 presents a typical solution with the cage friction coefficient of 0.15; note the general magnitude of the high peaks is 10 to 15 N. The force at the cage/race guide land varies in the same general range, however, the frequency of contact is quite large and as seen in Fig. 4, the contact is almost steady with a mean force of about 2.70 N. The cage whirls at a speed essentially equal to its angular velocity in an almost circular orbit, as shown in Figs. 5 and 6, respectively. Note that the operating clearance at the guide lands, after allowing for centrifugal expansion at the high speed, is 0.375 mm, which corresponds to the diameter of the cage orbit. Also, the mean force at

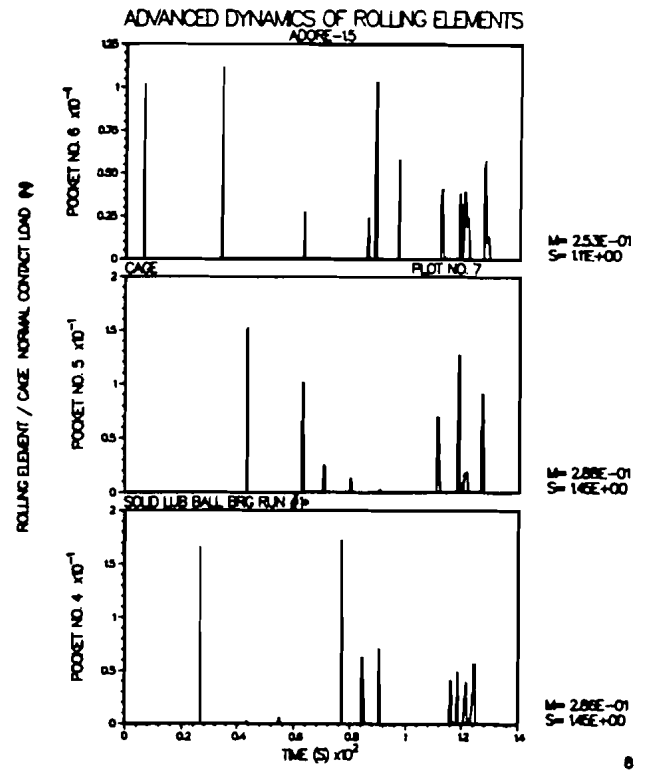


Fig. 3—Typical ball/cage interaction with a cage friction coefficient of 0.15.

the guide land, as seen in Fig. 4, is very close to the centrifugal force acting on the cage due to the whirl motion. This implies that the force at the guide lands is essentially independent of the magnitude of the pocket forces and is only related to the whirl velocity. Such an observation will generally be true whenever the cage has a definite whirl velocity.

Time-averaged wear rates, computed on the basis of the model discussed above are shown in Figs. 7 and 8, respectively, for the ball pockets and the guide lands. It is seen that the rates indeed show a trend of stabilization over the time domain over which the simulation is obtained. The steady-state wear rates derived from these figures may be used to compute the quantity of wear over a prescribed duty cycle of the bearing. Thus, significant insight into the wear distribution on the cage and overall wear life of the bearing may be obtained.

When the time-averaging algorithm is applied to the ball/race interaction, the wear rates for the races and the balls can also be computed. Figure 9 shows the wear rate for ball

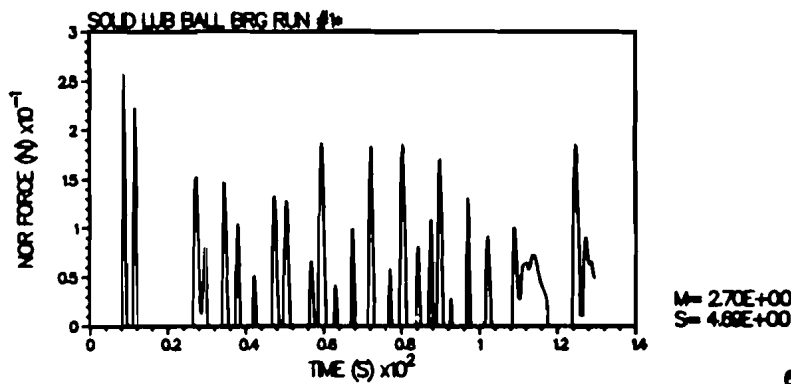
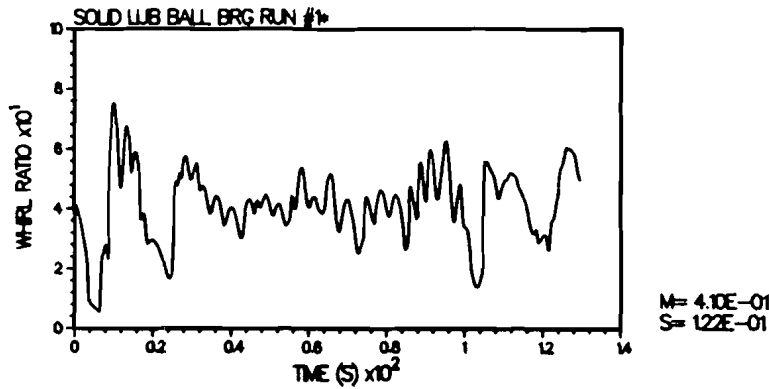


Fig. 4—The contact force variation at the cage/race guide land with a cage friction coefficient of 0.15



5

Fig. 5—Cage mass center whirl velocity with cage friction coefficient of 0.15

1, the two races, and the total wear rate for the cage, which is a sum of the wear rates in all pocket and the guide lands. Since all balls go through the same load cycle, the wear rates for all the balls are essentially identical. It must be noted,

however, that all wear rates are subject to the wear coefficients listed in Table 1. According to most wear theories, the ceramic balls may not wear at all and all the wear may take place on the steel races. In any event, if the actual wear coefficients are available from conventional wear tests, then the wear rates may be appropriately prorated.

ADVANCED DYNAMICS OF ROLLING ELEMENTS

ADORE-15

CAGE

PLOT NO. 5

SOLID LUB BALL BRG RUN #1

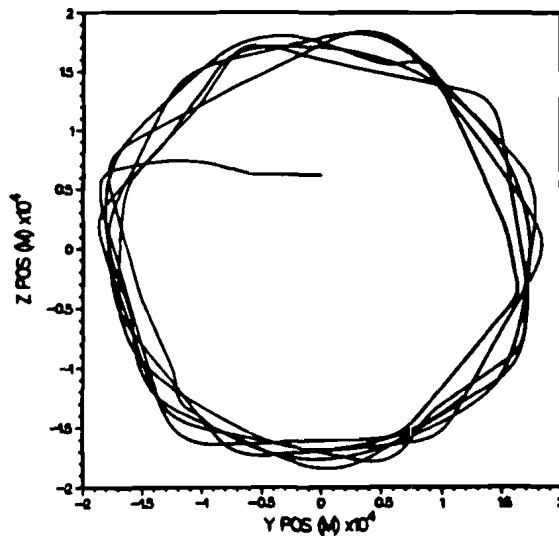


Fig. 6—The shape of cage whirl orbit with a cage friction coefficient of 0.15.

All of the results discussed thus far are obtained with the cage friction coefficient of 0.15. In order to see the effect of this friction coefficient, the simulation was repeated with the friction coefficient reduced to 0.050, which may represent a lower limit for most solid lubricants. Both the whirl velocity of the cage and the shape of the cage mass center orbit are unchanged with the lower friction; Fig. 10 shows the simulated mass center orbit. When Fig. 10 is compared to Fig. 6, it must be noted that the time domain for the simulation with the lower value of the friction coefficient is significantly larger and, therefore, the number of orbits in Fig. 10 is quite large when compared to those in Fig. 6. This difference essentially results from the numerical optimization of the time step size during integration of the equations of motion in ADORE; the smaller value of friction results in a larger permissible step size for the same limit on the local truncation error. In any case, the general shape of the orbits, when examined closely, are found to be identical for the two cases.

The overall level of ball/cage interactions is significantly reduced with the lower pocket friction and this results in a

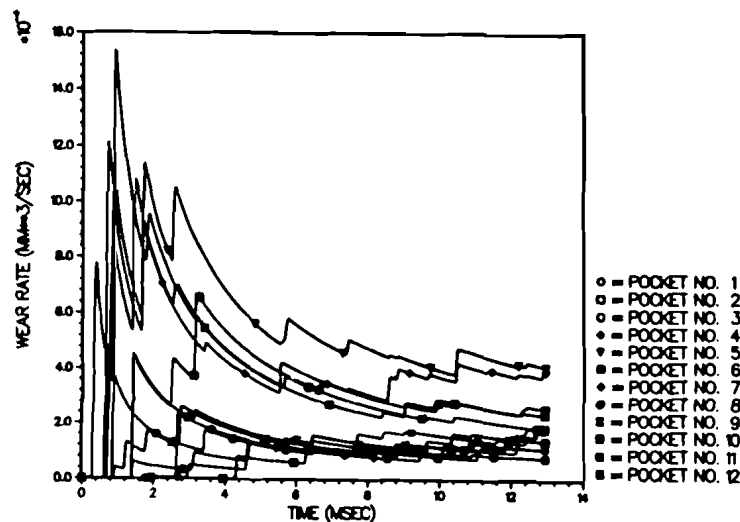


Fig. 7—Simulation of cage pocket wear with cage friction coefficient of 0.15

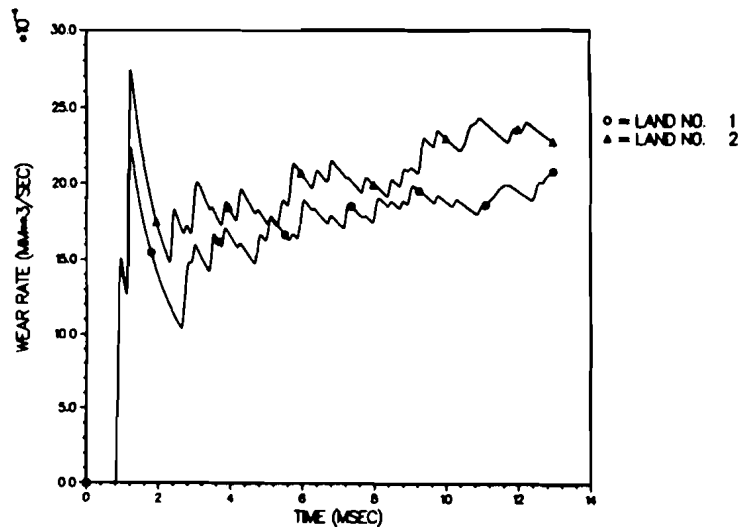


Fig. 8—Simulated wear rates at the cage/race guide lands with a friction coefficient of 0.15

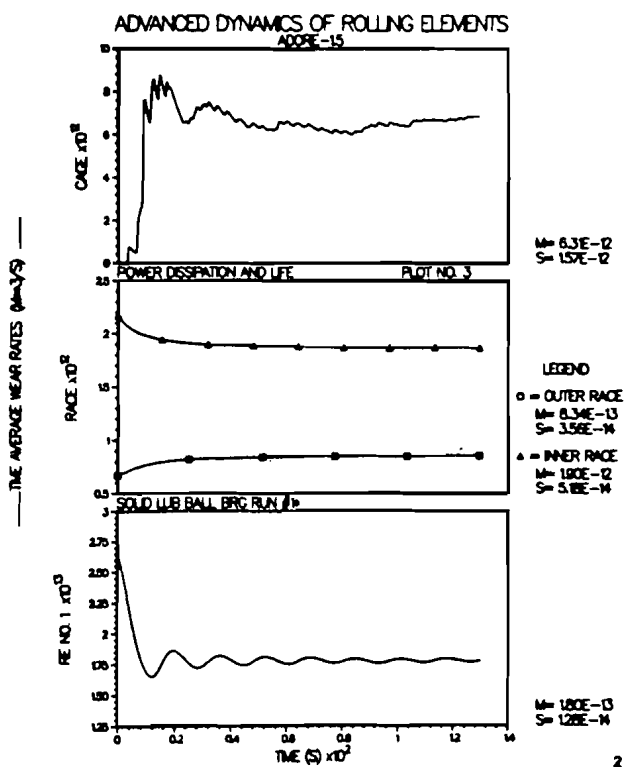


Fig. 9—Overall wear rates of the bearing elements with a cage friction coefficient of 0.15.

reduction of about a factor of two in the steady-state wear rates in cage pockets when compared to the results shown in Fig. 7. The interaction at the guide lands, however, is relatively unchanged. This is perhaps due to the fact that the guide land force is quite independent of the interactions in the cage pockets, and it only depends on the guide clearance and the whirl velocity, as discussed above.

The overall wear rates with the lower friction are shown in Fig. 11. Note the interesting finding that although the overall cage wear rate is lower with lower cage friction, there is a slight increase in the simulated wear rates of the balls and the races; compare Fig. 11 with Fig. 9. Further examination of the ball motion revealed that the ball/race slip is somewhat larger with the lower cage friction, which implies that the cage friction attempts to "damp" excessive ball/race slip; Fig. 12 compares the simulated ball/race ve-

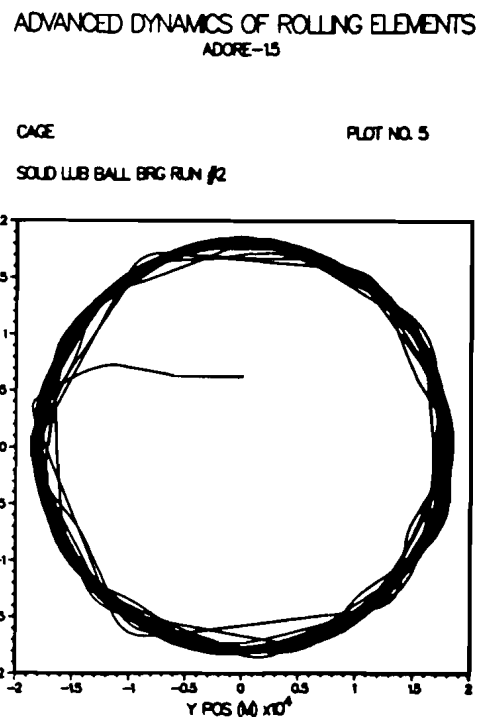


Fig. 10—Cage mass center orbit shape with a friction coefficient of 0.050

locities for the two values of cage friction. Indeed, further parametric evaluation as a function of both cage and ball/race friction, as well as experimental evidence, shall be necessary before the universal validity of such a finding can be substantiated.

As might be expected, the lower cage friction results in an overall reduction in the power loss, or heat generated, in the bearing, as shown in Fig. 13. Reduction in frictional dissipation at the ball/cage and cage/race contacts is quite large when compared to the small increase in the heat generated at the ball/race interface, due to a small increase in ball/race slip. This explains the overall lower power loss with the reduced cage friction.

CONCLUSIONS

A close integration of the constitutive wear relations, derived from conventional wear tests, with the dynamic models,

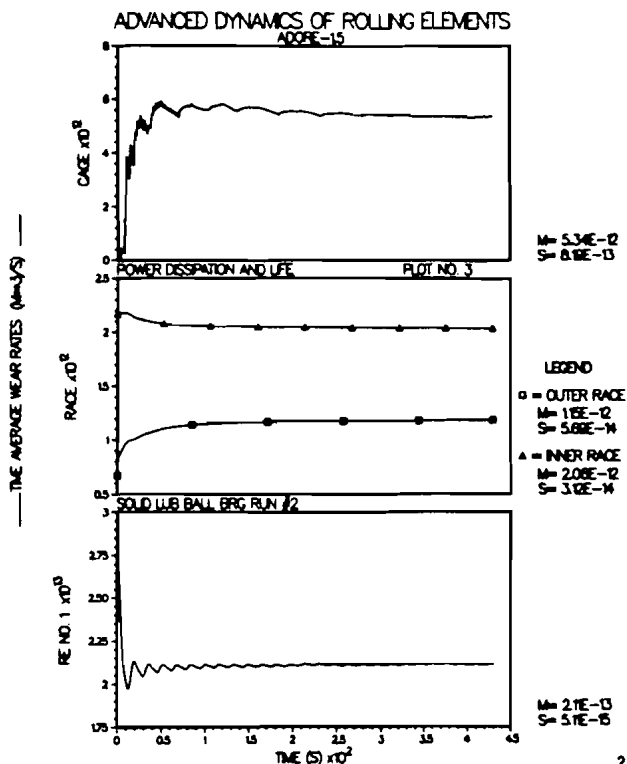


Fig. 11—Overall wear rates of the bearing elements with a cage friction coefficient of 0.050.

based on the classical equations of motion of the bearing elements, can result in a viable analytical model to predict wear in a ball bearing. A rigorous analysis of all interactions in the bearing provides wear distribution over each interaction. The modeling technique is thus significant for the

design of bearings for optimum material transfer and wear life of the bearing. The significance of the modeling technique is demonstrated for a solid-lubricated ball bearing operating at predicted gas turbine engine conditions.

ACKNOWLEDGMENTS

The research reported herein was sponsored by the Air Force Aero Propulsion Laboratory, Wright-Patterson Air Force Base, Ohio under the Defense Small Business Innovation Research Program, Contract Number F33615-84-C-2477. The computer services were provided by the ASD Computer Center at Wright-Patterson Air Force Base.

REFERENCES

- (1) Walters, C. T., "The Dynamics of Ball Bearings," *ASME J. Lubr. Technol.*, **93**, pp 1-10 (1971).
- (2) Gupta, P. K., "Dynamics of Rolling Element Bearings, Parts I to IV," *ASME J. Lubr. Technol.*, **101**, pp 293-326 (1975).
- (3) Gupta, P. K., "Simulation of Low-Frequency Components in the Dynamic Response of a Ball Bearing," *Advances in Computer-Aided Bearing Design, Proc. ASLE/ASME Lubr. Conf.* (1982).
- (4) Meeks, C. R. and Ng, K. O., "The Dynamics of Ball Separators in Ball Bearings, Part I-Analysis," *ASLE Trans.*, **28**, 3, pp 277-287 (1985).
- (5) Gupta, P. K., *Advanced Dynamics of Rolling Elements*, Springer-Verlag (1984).
- (6) Fehlberg, E., "Classical Fifth-, Sixth-, Seventh- and Eighth-Order Runge-Kutta Formulas with Step Size Control," NASA Technical Report, NASA TR R-287, George C. Marshall Space Flight Center, Alabama, October 1968.
- (7) Gupta, P. K., "Some Dynamic Effects in High-Speed Solid Lubricated Ball Bearings," *ASLE Trans.*, **26**, 3, pp 393-400 (1983).

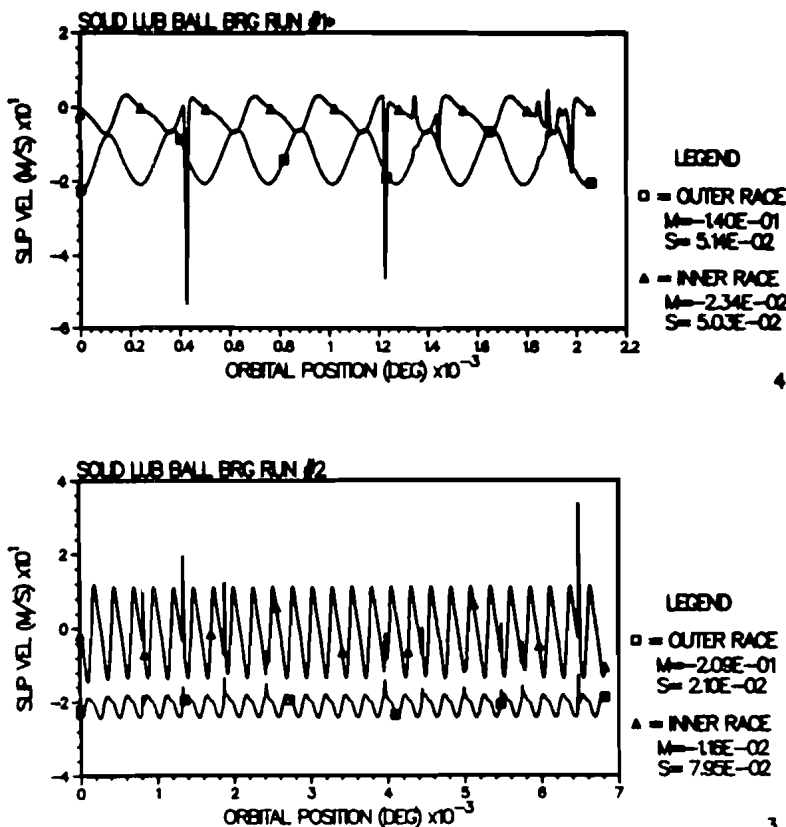


Fig. 12—Ball/race slip velocities as a function of cage friction.
 (a) Cage friction coefficient = 0.15
 (b) Cage friction coefficient = 0.050

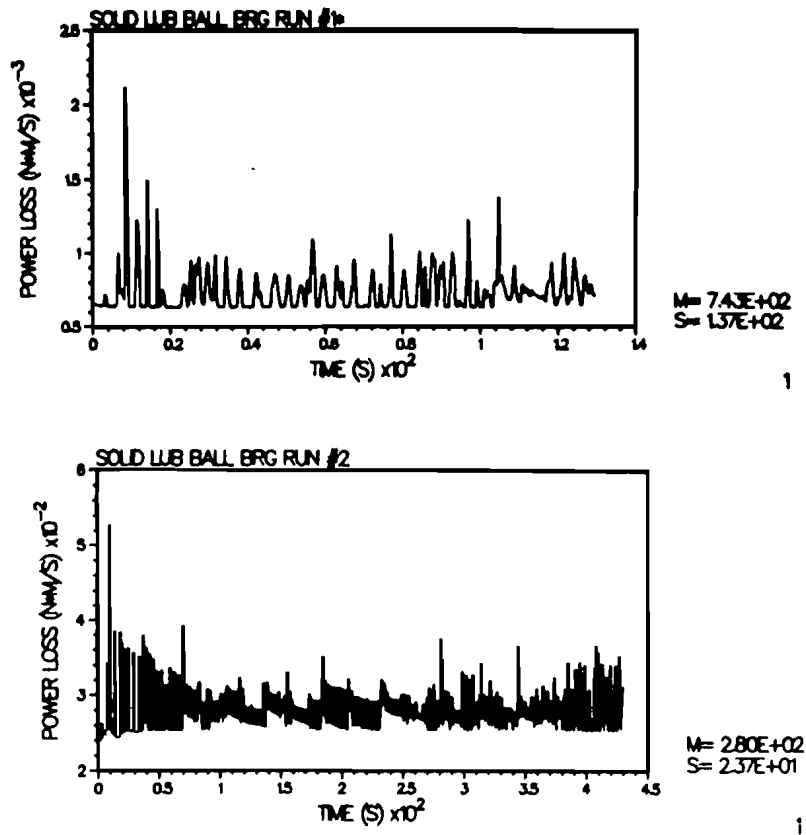


Fig. 13—Bearing power loss as a function of cage friction.

(a) Cage friction coefficient = 0.15

(b) Cage friction coefficient = 0.050

- (8) Bandow, H. E., Gray, S. E., and Gupta, P. K., "Performance Simulation of a Solid Lubricated Ball Bearing," ASLE Preprint No. 85-AM-4E-3, to be published in *ASLE Trans.*
- (9) Mecklenberg, K. R., "Lubricant Compact Wear Rate Techniques," Air

Force Materials Laboratory Report, AFWAL-TR-81-4014, Wright-Patterson Air Force Base, Ohio, 1981.

- (10) Meeks, C. R. and Bohner, J., "Predicting Life of Solid-Lubricated Ball Bearings," *ASLE Trans.*, 29, 2, pp 203-213 (1986).